Chin. Geogra. Sci. 2021 Vol. 31 No. 4 pp. 735−750
https://doi.org/10.1007/s11769-021-1221-9

Springer Science Press
www.springerlink.com/content/1002-0063

Risk Prevention and Control for Agricultural Non-Point Source Pollution Based on the Process of Pressure-Transformation-Absorption in Chongqing, China

ZHU Kangwen[1], CHEN Yucheng[1, 2], ZHANG Sheng[3], YANG Zhimin[1, 2], HUANG Lei[1, 2], LEI Bo[3], XIONG Hailing[4], WU Sheng[4], LI Xixi[5]

(1. *College of Resources and Environment*, *Southwest University*, *Chongqing* 400716, *China*; 2. *Chongqing Engineering Research Center of Rural Cleaning*, *Chongqing* 400716, *China*; 3. *Chongqing Academy of Ecology and Environmental Sciences*, *Chongqing* 401147, *China*; 4. *College of Computer & Information Science*, *Southwest University*, *Chongqing* 400716, *China*; 5. *Chongqing Chemical Industry Vocational College*, *Chongqing* 401220, *China*)

Abstract: According to China's second national survey of pollution sources, the contribution of agricultural non-point sources (ANS) to water pollution is still high. Risk prevention and control are the main means to control costs and improve the efficiency of ANS, but most studies directly take pollution load as the risk standard, leading to a considerable misjudgment of the actual pollution risk. To objectively reflect the risk of agricultural non-point source pollution (ANSP) in Chongqing, China, we investigated the influences of initial source input, intermediate transformation, and terminal absorption of pollutants via literature research and the Delphi method and built a PTA (pressure kinetic energy, transformation kinetic energy, and absorption kinetic energy) model that covers 12 factors, with the support of geographical information system (GIS) technology. The terrain factor calculation results and the calculation results of other factors were optimized by Python tools to reduce human error and workload. Via centroid migration analysis and Kernel density analysis, the risk level, spatial aggregation degree, and key prevention and control regions could be accurately determined. There was a positive correlation between the water quality of the rivers in Chongqing and the risk assessment results of different periods, indirectly reflecting the reliability of the assessment results by the proposed model. There was an obvious tendency for the low-risk regions transforming into high-risk regions. The proportion of high-risk regions and extremely high-risk regions increased from 17.82% and 16.63% in 2000 to 18.10% and 16.76% in 2015, respectively. And the risk level in the main urban areas was significantly higher than that in the southeastern and northeastern areas of Chongqing. The centroids of all grades of risky areas presented a successive distribution from west to east, and the centroids of high-risk and extremely high-risk regions shifted eastward. From 2000 to 2015, the centroids of high-risk and extremely high-risk regions moved 4.63 km (1.68°) and 4.48 km (12.08°) east by north, respectively. The kernel density analysis results showed that the high-risk regions were mainly concentrated in the main urban areas and that the distribution of agglomeration areas overall displayed a transition trend from contiguous distribution to decentralized concentration. The risk levels of the regions with a high proportion of cultivated land and artificial surface were significantly increased, and the occupation of cultivated land in the process of urbanization promoted the movement of the centroids of high-risk and extremely high-risk regions. The identification of key areas for risk prevention and control provides data scientific basis for the development of prevention and control strategies.

Keywords: geographic information system (GIS); agricultural non-point source pollution (ANSP); risk assessment; Kernel density; Chongqing; China

Citation: ZHU Kangwen, CHEN Yucheng, ZHANG Sheng, YANG Zhimin, HUANG Lei, LEI Bo, XIONG Hailing, WU Sheng, LI Xixi, 2021. Risk Prevention and Control for Agricultural Non-Point Source Pollution Based on the Process of Pressure-Transformation-Absorption in Chongqing, China. *Chinese Geographical Science*, 31(4): 735−750. https://doi.org/10.1007/s11769-021-1221-9

Received date: 2020-10-26; accepted date: 2021-01-06

Foundation item: Under the auspices of the Chongqing Science and Technology Commission (No. cstc2018jxjl20012, cstc2018jszx-zdyfxmX0021, cstc2019jscx-gksbX0103)

Corresponding author: CHEN Yucheng. E-mail: cyc_sw_edu@163.com; ZHANG Sheng. zs_hky@163.com

1 Introduction

Agricultural non-point source pollution (ANSP) refers to water pollution caused by nitrogen, phosphorus, pesticides, and other pollutants through farmland runoff and leachate (Smith and Siciliano, 2015). In the prevention and control of water pollution in China, point sources are mainly considered, whereas non-point sources have long been ignored (Liu et al., 2005). However, with the effective control of point source pollution, increasing attention has been paid to ANSP. According to the results of the second general survey of pollution sources in China (Liu et al., 2020; Wang et al., 2020), the total discharge of water pollutants decreased significantly from 2007 to 2017, the chemical oxygen demand (COD), total nitrogen (TN), and total phosphorus (TP) in 2007 and 2017 were 3028.96, 472.89, 42.32 and 2143.98, 304.14, 31.54 million t, respectively. While the proportions of agricultural sources in COD, TN, and TP emissions from 43.71%, 41.88%, and 67.27% to 49.77%, 40.73%, and 67.22%, respectively, indicating that the contribution of ANSP to water pollution is still high. Chongqing, China is characterized by hilly and mountainous landforms, fractured landforms, a high proportion of rural areas in the urban-rural dual structure, hot rainy seasons, and concentrated precipitation, resulting in a large potential threat, wide coverage, and large driving energy of ANSP in this region (Li et al., 2018; Zhou et al., 2019). According to the Chongqing data system (http://www.cqdata.gov.cn/), the application amount of chemical fertilizers and pesticides in Chongqing is relatively high, reaching 278.24, and 18.45 kg/ha, respectively, in 2018. These values largely exceed the international safety thresholds. The multiple cropping index of agricultural land in Chongqing is high (Sun et al., 2017). In addition, the impacts of topography and climate on soil erosion are also nonnegligible. Chongqing is located in the center of the Three Gorges Reservoir area and represents the connecting point between 'One Belt And One Road' and the Yangtze River economic belt and therefore holds an important position in the national regional development pattern; it is also an important ecological barrier in the upper reaches of the Yangtze River. In this sense, strict water resource management strategies are indispensable. To ensure the ecological security of the Yangtze River basin, the problem of ANSP needs to be solved.

The premise to effectively solve the problem of ANSP is to accurately assess the distribution of risk status, the risk level, and the risk evolution of such pollution. In particular, the integration of various technologies and methods, such as the ANSP calculation model (Hou et al., 2014), the universal soil loss equation (USLE) (Shen et al., 2009), and GIS technology (Basnyat et al., 2000), have greatly promoted research on ANSP in China (Wang et al., 2019). At present, the measurement of ANSP risks is afflicted with the following issues: 1) many studies have confused the risk measurement of ANSP with load measurement or have even equated these two approaches. Generally, the pollution load is the result of theoretical calculations based on pollution discharge, while the pollution risk is the result of actual estimations based on comprehensive consideration of pollutant transmission means. If the load calculation result is simply viewed as the risk level result, there will be misjudgment of the risk degree of ANSP (Wang et al., 2017). Therefore, it is necessary to construct a measurement method that can objectively reflect the risk degree of regional non-point source pollution (NSP); 2) there are few studies on the spatio-temporal evolution of ANSP risk. In terms of risk assessment, the most commonly used technical methods include the output coefficient method (Cai et al., 2018), the pollution index method (phosphorus index method) (Ouyang et al., 2012), the multi-factor index evaluation method (Mao et al., 2002), and the NSP model evaluation method (Strehmel et al., 2016), but there are few studies on the combination of agricultural and geographical methods; 3) in the risk assessment of ANSP, many studies consider source input and terminal absorption (Xu et al., 2018), but few studies consider the intermediate transformation dimensions. For example, Jiang et al. (2018) carried out the environmental risk analysis of farmland nutrient balance, which was focused on the input intensity of nitrogen and phosphorus and nutrient absorption. Scholars have carried out some researches on these problems. Wu et al. (2020) used the phosphorus index model to calculate the risk of phosphorus loss from farmland in Haihe River Basin, China, and took the soil erosion modulus, annual runoff depth, normalized distance index between farmland and water body involved in the process of phosphorus loss as migration factors.

Kang et al. (2018) assessed the risk of nitrogen and phosphorus loss from farmland surface runoff combined with GIS, and analyzed the rainfall and river network density. De Oliveira et al. (2017) proposed to use land cover pollution index combined with water quality data to simulate non-point source pollution in Brazilian watershed. All of these studies integrated geographical methods into agronomic analysis, and considered the transformation process of pollutants to a certain extent. These studies provide a good reference for our research.

Based on the above problems and the existing researches, in order to accurately identify the distribution, evolution and key areas of ANSP risk in Chongqing, firstly, considering the impact of pollutant source input, process conversion and terminal absorption, a model was constructed based on GIS technology, which included pressure kinetic energy, transformation kinetic energy, and absorption kinetic energy (PTA model). Secondly, the movement trend of high-risk and extremely high-risk regions of ANSP was studied by using the method of centroid analysis. Thirdly, the kernel density analysis method was used to identify the high-risk and extremely high-risk regions in different periods. Finally, the accuracy of risk assessment, influencing factors and prevention-control suggestions of ANSP were discussed. We hope to provide reference for risk identification and risk prevention-control of ANSP, and solve the problem that ANSP covers a wide range while difficult to accurately identify high-risk areas.

2 Research methods

2.1 Study area

Chongqing is the only municipality directly under the Central Government in the western China. According to the Chongqing data system in 2018 (http://www.cqdata.gov.cn/), there are 27 counties with fertilizer application intensity over 225 kg/ha and 31 counties with pesticide application intensity over 2.5 kg/ha in Chongqing. Therefore, the current level of fertilizer application in Chongqing is far higher than the internationally recognized safe upper limit. And the livestock and poultry stocking rates are greatly increasing. The proportion of mountainous and hilly landforms in Chongqing's administrative area is 75.8% and 15.2%, respectively (Zhang et al., 2019). Precipitation in Chongqing is heavy and concentrated, and the area subjected to soil erosion accounts for 48.6% of the total area (Sun et al., 2017). According to the analysis of land use changes in Chongqing from 2000 to 2015, the land use areas of various land types have changed significantly (Fig. 1). Construction land, forest land, grassland, and water area have been in a state of continuous increase, while the cultivated land has continuously decreased; other land use types show a fluctuating trend. In 2000, 2005, 2010, and 2015, the area percentages of the land use types (construction land, forest land, grassland, water area, cultivated land, and other land) in total land area were shown in Table 1. Based on land use change data, urbanization and environmental protection have been promoted in a coordinated way in the past. From the perspective of spatial distribution, there is a relatively obvious trend of the expansion and concentration of construction land and the gradual increase in the coverage rates of forest land and grassland. The construction land area is mainly expanded and concentrated in the main urban areas, while construction land expands relatively slowly in the northeastern and southeastern Chongqing, where the focus is on ecological protection. To sum up, the combination of land use types, topography, climate conditions, fertilizer and pesticide applications, and other regional conditions leads to the intensification of ANSP in Chongqing.

2.2 Methods

In this context, considering previous research results and the regional characteristics of Chongqing (Wang et al., 2016; Zhou et al., 2019), we combined the conventional methods in the field of ANSP with a geographical approach, referring to the local standard of Chongqing, i.e., '*Technical Specification for Chongqing Agricultural Non-point Source Pollution Risk Assessment*' (DB50/T 931−2019, Chongqing Market Supervision and Administration Bureau, 2019. http://dbba.sacinfo.org.cn/stdDetail/7096b8466aef373cc71ee926072d76f7cd7c5e16a3612a1f2d5c67b09aef4790), and employing the quantitative method and the Delphi method for rounds of soliciting experts' suggestions to determine the risk measure index (Strand et al., 2017). To objectively reflect the risk level of ANSP, we considered the influences of pollutant source input, intermediate transformation, and terminal absorption and constructed the

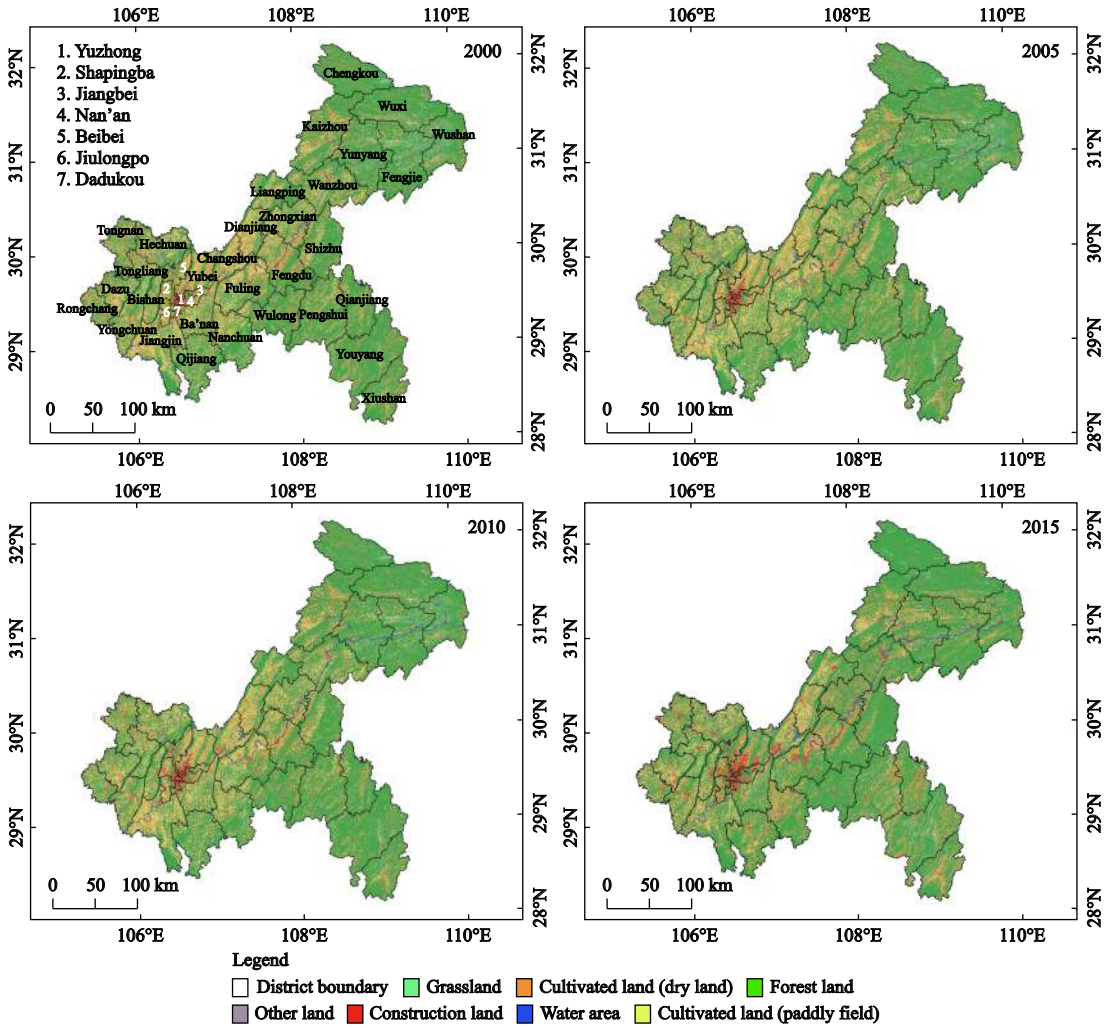

Fig. 1 Distribution of land use types from 2000 to 2015 in Chongqing, China. The land use data were derived from the Chinese Ecological Environment Remote Sensing Assessment Project (Ouyang et al., 2014; 2016)

Table 1 The area percentages (%) of the land use types in total land area from 2000 to 2015 in Chongqing, China

Land use types	2000	2005	2010	2015
Construction land	1.05	1.41	1.71	3.18
Forest land	54.2	55.03	56.07	57.94
Grassland	2.52	2.57	2.85	3.85
Water area	1.4	1.59	1.79	1.96
Cultivated land	40.74	39.35	37.71	33.03
Other land	0.09	0.05	0.02	0.04

model covering 12 factors in three dimensions of pressure kinetic energy, transformation kinetic energy, and absorption kinetic energy, with the support of GIS technology. The pressure kinetic energy mainly considers the source input, such as the conventional fertilizer intensity index, the pesticide intensity index, and the livestock and poultry breeding intensity index. At the same time, considering the actual situation of ANSP, the pressure kinetic energy introduces the aquaculture index, which is usually ignored, and the residential intensity, which reflects the degree of human interference. Kinetic energy transformation mainly considers the impacts of the natural environment on pollutant transportation, including the rainfall erodibility index, the slope length and gradient index, the sloping farmland index, the soil erodibility index, and the water area distance index. Absorption kinetic energy mainly considers the terminal interception and absorption, including the forest and grass retention index, which reflects the interception capacity of forest and grass land to pollutants, and the water capacity index, reflecting the capacity of waterbodies.

Based on the construction of the PTA model, this re-

search optimizes the algorithms of relevant indices. The involved pressure kinetic energy indices were spatialized according to the land use type distribution to reflect the spatial differences; the slope length and gradient index was calculated to obtain the optimal window by Python programming; the soil erodibility was measured using the EPIC model rather than the commonly used direct assignment method based on soil types; the absorption kinetic energy index was calibrated by the calculation results of kernel density. Our research results have the advantages of high visibility of risk assessment results, identifiable risk levels, and analyzable risk variation. Via centroid motion analysis and kernel density analysis, the results can be well analyzed to better reflect the spatial differences. Thus, the problem of wide coverage ranges of ANSP but high difficulty in accurate identification of the high-risk regions can be solved (Rabotyagov et al., 2014; Karandish and Šimůnek, 2017).

2.2.1 Construction of the PTA Model to determine the ANSP risk

To ensure the scientificity of the subjective weighting method, the Delphi method was used to solicit opinions on the selected factors and their weights. The essential meaning of the weight is the influence degree of a certain assessment index on the assessment results and the degree of people's attention to the index, of which the former reflects the objectivity of the weight and the latter the subjectivity of the weight. The questionnaire was designed according to the actual circumstances of the study area. We solicited opinions from 72 experts of agriculture and rural departments, environmental departments, natural resources departments, colleges and universities, and research institutes. After two rounds of opinion solicitation, we used related formulas to obtain the selection frequency of different importance values and the weight of each index (Table 2). According to 20%, 40%, 60% and 80% of the total comprehensive index, the risk measurement results of ANSP can be divided into five grades: no risk, low risk, medium risk, high risk and extremely high risk.

To calculate the weight of the assigned score for each index from each expert, we used the following equation:

$$a_i = \frac{q_i}{\sum_{i=1}^{m} qi} \tag{1}$$

where a_i is the weight of the assigned score for a certain index from a certain expert; q_i is the score assigned by an expert to this index; m is the number of the indices for ANSP risk assessment.

We used the following formula to calculate the proportion of each index and the difference degree of the assigned scores for each index by the experts:

$$p = \frac{\sum_{i=1}^{n} q_i}{n} \tag{2}$$

$$g = \frac{\sum_{i=1}^{n} (q_i - p)^2}{n} \tag{3}$$

where p is the weight of each assessment index assigned by the experts; g is the difference degree of the scores assigned by experts to various indices (the smaller the value of g, the closer the assigned score); q_i is the score assigned by a certain expert to this index; n is the number of experts participating in the assignment of the assessment index.

2.2.2 Centroids of high-risk regions

The high-risk region centroid (X, Y) is defined as the centroid position of high-risk areas of ANSP. The centroid theory has been well applied in population, energy, economy, industry, and tourism sciences, among others, and the change of the centroid position can reflect the changes of the spatial distribution of ANSP risks (Wu et al., 2014; Liu et al., 2017). The centroid offset distance Δ_t refers to the movement distance of the ANSP risk during a certain research period, and the offset angle α_t refers to the included angle between the movement direction of the centroid of different levels of risk areas and the due east direction during the research period. The average offset velocity V_t refers to the average movement speed of centroid of different levels of risk areas during the research period. The equation is as follows:

$$\Delta_t = \sqrt{(X_t - X_{t-1})^2 + (Y_t - Y_{t-1})^2} \tag{4}$$

$$\alpha_t = n\pi + \arctan\left(\frac{Y_t - Y_{t-1}}{X_t - X_{t-1}}\right), (n = 0, 1, 2) \tag{5}$$

$$V_t = \Delta_t / T \tag{6}$$

where (X_t, Y_t) and (X_{t-1}, Y_{t-1}) are the coordinates of the centroids of different levels of risk areas of ANSP in the

Table 2 The implications, levels and weights of indices in PTA model of agricultural non-point source pollution (ANSP) risk measurement in Chongqing, China

Index	Index implications	Extremely high risk	High risk	Medium risk	Low risk	No risk	Weight
I_1	Kinetic energy of ANSP released by source input in space						0.38
I_2	Kinetic energy of ANSP released by intermediate transformation in space						0.32
I_3	Kinetic energy of ANSP released by terminal absorption in space						0.30
I_{11}	Fertilizer input pressure per unit area of cultivated land	> 280	250−280	225−250	200−225	≤ 200	0.24
I_{12}	Pesticide input pressure per unit area of cultivated land	> 4	3.5−4.0	3.0−3.5	2.5−3.0	≤ 2.5	0.21
I_{13}	Discharge pressure from livestock breeding pollutants	> 2	1−2	0.500−1	0.300−0.500	≤ 0.300	0.22
I_{14}	Discharge pressure from aquaculture pollutants						0.18
I_{15}	Discharge pressure from residential pollutants caused by dense rural houses and township roads	> TI_i× 0.8	TI_i×0.6−TI_i×0.8	TI_i×0.4−TI_i×0.6	TI_i×0.2−TI_i×0.4	≤ TI_i×0.2	0.15
I_{21}	Soil erosion ability driven by rainfall	> 600	400−600	100−400	25−100	≤ 25	0.22
I_{22}	Water and soil loss caused by large-scale topographical movement	> 300	100−300	50−100	20−50	≤ 20	0.19
I_{23}	Water and soil loss caused by microscopic topographical movement	> 25	20−25	15−20	5−15	≤ 5	0.18
I_{24}	Water erosion resistance caused by soil property differences	0.020−0.040	0.015−0.020	0.011−0.015	0.007−0.011	≤ 0.007	0.20
I_{25}	Spatial resistance of pollutants to the receiving water	> 5000	2000−5000	1000−2000	500−1000	≤ 500	0.21
I_{31}	Active absorptive capacity of forest and grass areas to pollutants						0.52
I_{32}	Passive absorptive capacity of receiving water to pollutants	≤ TI_i×0.2	TI_i×0.2−TI_i×0.4	TI×0.4−TI_i×0.6	TI_i×0.6−TI_i×0.8	> TI_i×0.800	0.48
Assigned score		5	4	3	2	1	

Note: I_i represents the index of each involved in the measurement, and i refers to the number of index. TI_i represents the total measured results of the I_i index, and the grading method refers to the grading idea of ecosystem service function importance assessment. The segmented values corresponding to the cumulative percentages of 20%, 40%, 60%, and 80% were obtained by Python programming. **The grading principles are as follows:** 1) I_{11}: According to the index system of constructing ecological civilization demonstration towns and demonstration villages in Chongqing (Sun et al., 2014), the fertilizer use risk value is 280 kg/a; according to the index system of constructing state-level ecological towns and counties (Zhang et al., 2016), the fertilizer use risk value is 250 kg/a; the upper safety limit of fertilizer use in the developed countries is 225 kg/ha (Liu, 2014); according to the study of Zhang et al. (2008a; b), crop fertilizer use of more than 200 kg/hm^2 means a high risk level. 2) I_{12}: The internationally recognized safe use level of pesticide intensity is 2.5 kg/a, and the risk levels are graded according to relevant studies on ecosystem health assessment (Zhu et al., 2019). 3) I_{13}: The total amount of livestock manure resources and the manure load of cultivated land are calculated by using the *Technical Guide for Calculating the Carrying Capacity of Livestock and Poultry Manure* (Ministry of Agriculture and Rural Affairs of the People's Republic fo China, 2018, http://www.moa.gov.cn/nybgb/2018/201802/201805/t20180515_6142139.htm). The regional environmental risks of livestock and poultry manure were assessed in combination with the nutrient requirements of regional crop manure and graded into five levels, based on the research of Xiao et al. (2019). 4) I_{14}: This index can be calculated by using the distribution kernel density of small reservoirs and the aquatic production per unit area. 5) I_{15}: This is composed of the density of rural houses and township roads. The density of rural houses reflects the interference degree of human activities in rural areas and the living emission intensity of rural residents. The density of township roads reflects the unimpeded flow of human activities and the frequency of visits. 6) I_{21}: The currently accepted daily precipitation erodibility model is used to calculate the monthly rainfall erodibility, and the annual precipitation erodibility is calculated according to the monthly precipitation erodibility (units: (MJ·mm)/(ha·h·yr)). This index is graded according to the algorithm of soil erosion sensitivity in *Ecological Function Zoning* (Li et al., 2013). 7) I_{22}: Python programming is used to calculate the optimal calculation window of slope length and slope gradient (Zhong and Lu, 2018), and slope length and gradient are graded according to the algorithm of soil erosion sensitivity in *Ecological Function Zoning* (unit: m). 8) I_{23}: This index is assessed according to the grading levels for slope gradient in *Ecological Function Zoning* (unit: °). 9) I_{24}: Soil erodibility is closely related to soil mechanical composition and soil organic carbon content. The EPIC (Environmental Policy-Integrated Climate) model (WILLIAMS et al., 1983) is widely used for soil erodibility measurement (unit: (t·ha·h)/(MJ·hm^2·mm)). This index is graded according to the research results for Chongqing by Zuo et al. (2010). 10) I_{25}: This index is graded according to the requirements of the delineation scope of drinking water source protection zone, the waterbody protection scope of livestock and poultry breeding zone, the waterbody protection scope of the Yangtze River Economic Belt, and the construction of the ecological corridor (unit: m). 11) I_{31}: This index is comprehensively measured according to the ratio of 'sink' to 'source' areas and the kernel density of 'sink' areas. 12) I_{32}: This index is comprehensively measured according to the index of water network density and the kernel density of water distribution. PTA, pressure kinetic energy, transformation kinetic energy, and absorption kinetic energy

*t*th and (*t*−1)th year respectively, and *T* is the time interval. Due to the range of arctangent function is (−π/2, π/2), the value needs to be converted to 0−360°, and *n* is the conversion coefficient.

2.2.3 Kernel density

Kernel density is a spatial analysis tool based on non-parametric testing (Wang and Zambom, 2019). The basic idea of element-oriented kernel density estimation is to assume that there is an element density at any given arbitrary location within a particular region. Then, the density intensity of geographical elements in a particular region can be estimated by measuring the number of elements per unit area, and the relative concentration degree of the spatial distribution of elements and the distribution of hotspot regions can be depicted by determining the element density at different locations and the spatial difference (Okabe et al., 2009; Kristan and Leonardis, 2014). The kernel density analysis tool in ArcGIS software is used to analyze the grids with high and extremely high risk levels to explore the limit position of ANSP risk in Chongqing.

2.3 Data sources

The data types are mainly divided into panel data, remote sensing data, and statistical data. The remote sensing data include land use data, soil type and texture data, digital elevation model (DEM) topographic data, slope data, river data, and road data for 2000, 2005, 2010, and 2015. Land use data were derived from the Chinese Ecological Environment Remote Sensing Assessment Project (Ouyang et al., 2014; 2016) and the latest data was in 2015. DEM data were from the resources and environmental data cloud platform (http://www.resdc.cn/). By using DEM data in the GIS software, the slope data can be calculated. River and road data, with a unified data resolution of 30 m, were extracted from high-resolution remote sensing images. Statistical data included fertilizer use data, pesticide use data, crop planting area data, livestock and poultry breeding data, and aquaculture data. Fertilizer use data, pesticide use data, and crop planting area data were derived from the Chongqing data system (http://www.cqdata.gov.cn/), livestock and poultry breeding data from the Chongqing Agriculture and Rural Committee (http://nyncw.cq.gov.cn/), and aquaculture data from the statistical results of the Chongqing Aquatic Product Station.

3 Results

3.1 Measured ANSP risks in Chongqing

According to the risk measurement results provided by the PTA model, the 'no risk' proportions of ANSP in Chongqing in 2000, 2005, 2010, and 2015 were 26.06%, 26.11%, 25.42%, and 24.86%, respectively. The 'low risk' proportions were 20.52, 20.58, 20.61, and 20.87, respectively, and the 'medium risk' proportions were 18.97%, 19.01%, 19.34%, and 19.41%, respectively. The 'high risk" proportions were 17.82%, 17.81%, 17.98%, and 18.10%, respectively, and the 'extremely high risk' proportions were 16.63%, 16.49%, 16.65%, and 16.76%, respectively. Overall, except for the decreasing proportion of the 'low risk' area, the proportions of other risk levels all presented an increasing trend, indicating that there is a relatively obvious transformation trend from low to high risk. Spatially, the risk level in the main urban areas was considerably higher than that in the southeast and northeast of Chongqing. The overall trend for different years was consistent, but there were differences in some districts and counties. In general, the proportions of high- risk and extremely high-risk areas in Tongliang, Yongchuan, Bishan, Shapingba, Beibei, North of Jiangjin, Fuling, Nanchuan, Qijiang and Fengdu were large, and the distribution of high-risk and extremely high-risk areas was relatively concentrated; the risk levels of Liangping, Kaizhou, Qianjiangand Pengshui increased significantly in 2015 (Fig. 2).

3.2 Changes in the centroids of risk areas

By measuring the centroids of all risk levels and their movement status in different periods, we found that the centroids of extremely high-risk, high-risk, medium-risk, low-risk, and no-risk areas of ANSP in Chongqing presented a successive distribution from west to east. From the perspectives of movement speed and migration angle, from 2000 to 2015 (in which periods A, B, and C represent 2000−2005, 2005−2010, and 2010−2015), the distribution of no-risk areas showed a fluctuating westward migration, and the fastest movement speed of the no-risk level appeared in period B. The distribution of low-risk areas showed a westward migration, and the fastest movement speed of such areas occurred in period B. Medium-risk areas showed a fluctuating westward migration, with the fastest movement in period B. The distribution of high-risk areas showed

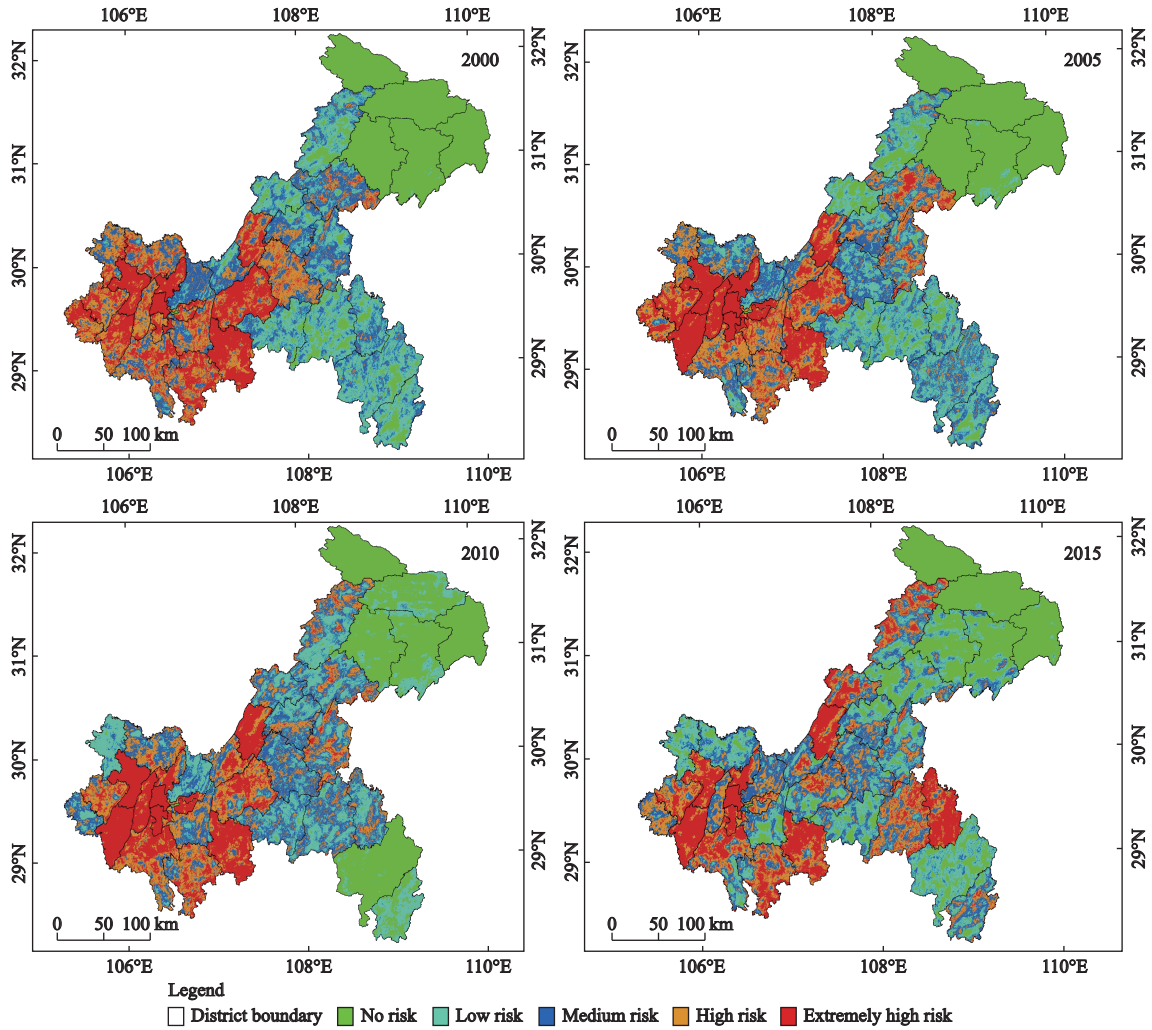

Fig. 2 Measurement results of risk of agricultural non-point source pollution (ANSP) from 2000 to 2015 in Chongqing, China

an obvious eastward migration, and the fastest movement speed of such areas was found for period A. Areas with an extremely high risk migrated eastward, and the fastest movement occurred in period C. Overall, medium- and low-risk areas showed a westward migration, and high- and extremely-high areas showed an eastward migration (Table 3, Table 4). From 2000 to 2015, the centroids of high-risk and extremely high-risk regions moved 4.63 km (1.68°) and 4.48 km (12.08°) east by north, respectively (Table 3, Table 4).

3.3 Kernel density of high risk and extremely high risk area

Kernel density analysis was mainly conducted for high

Table 3 Centroid coordinates of different risk levels in different periods of Chongqing (Unit: m)

Risk level	2000		2005		2010		2015	
	X	*Y*	*X*	*Y*	*X*	*Y*	*X*	*Y*
No risk	36603421	3434380	36598076	3440050	36604896	3391193	36584755	3422907
Low risk	36530127	3288016	36515514	3290823	36506810	3329510	36493427	3305019
Medium risk	36469415	3305356	36471970	3287238	36462930	3311908	36460792	3301214
High risk	36390317	3286472	36414422	3286700	36427717	3296636	36436579	3287826
Extremely high risk	36374127	3269800	36370296	3277248	36373569	3271017	36417973	3279184

Note: In order to calculate the offset direction and offset angle, the centroid coordinates are measured by projection coordinates

Table 4 Movement status of different agricultural non-point source pollution (ANSP) risk levels in different periods in Chongqing in 2000−2015

Risk level	2000−2005			2005−2010			2010−2015		
	Average movement speed / (m/yr)	Offset direction	Offset angle / (°)	Average movement speed / (m/yr)	Offset direction	Offset angle / (°)	Average movement speed / (m/yr)	Offset direction	Offset angle / (°)
No risk	1558.24	West by north	46.69	9865.97	East by south	82.05	7513.68	West by north	57.58
Low risk	2976.09	West by north	10.87	7930.85	West by north	77.32	5581.94	West by south	61.35
Medium risk	3659.36	East by south	81.97	5254.83	West by north	69.88	2181.13	West by south	78.70
High risk	4821.34	East by north	0.54	3319.33	East by north	36.77	2499.21	East by south	44.83
Extremely high risk	1675.09	West by north	62.78	1407.59	East by south	62.29	9029.69	East by north	10.42

risk and extremely high risk levels, with the purpose to spatially identify the concentration locations and the concentration degrees of high risk and extremely high risk levels (Fig. 3). According to the kernel density results, high-risk level areas were mainly distributed in the main urban areas, of which the north of Chongqing showed a relatively low risk concentration degree in different periods, while the risk concentration degrees of Tongnan, Hechuan, and Banan gradually decreased. Northeastern and Southeastern of Chongqing had a

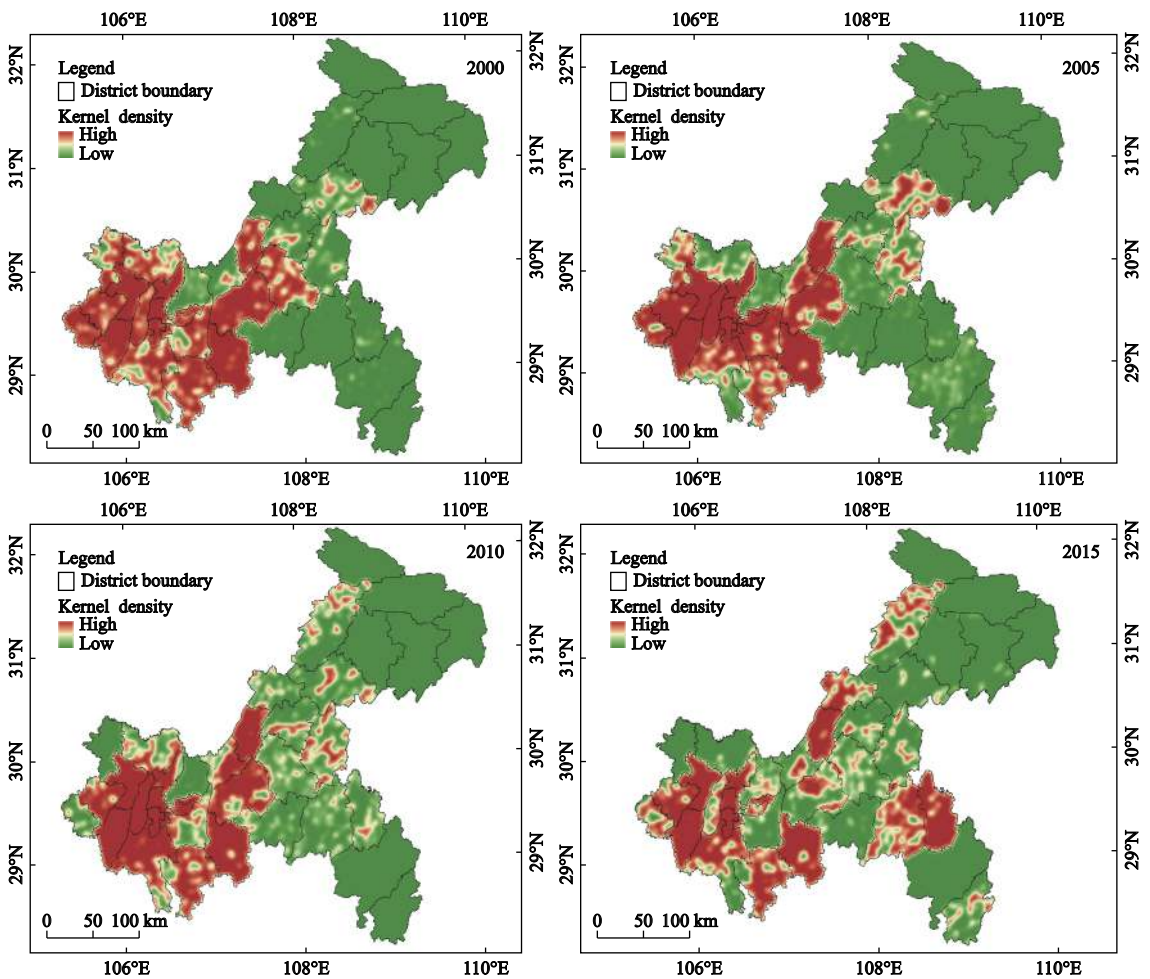

Fig. 3 Kernel density distribution of high- and extremely high-risk areas of ANSP in different periods in Chongqing, China

lower risk concentration degree, albeit with an increasing trend. We observed the concentrated distribution of high-risk areas in Dianjiang, Fengdu, and Wanzhou, with a particularly high concentration in Pengshui, Qianjiang, Kaizhou, and Liangping in 2015. In addition, overall, the spatial integrity of the concentrated distribution areas decreased while the fragmentation degree increased, showing a trend of gradual decentralized concentration.

3.4 Identification of key areas for risk prevention and control

According to the risk measurement process, the key areas for risk prevention and control should be understood as the key prevention areas (those areas with high risk intensity but good water quality, of which the risk level of ANSP is high or extremely high, and the water quality level is I-III) and the key control areas (areas with high risk intensity but poor water quality, of which the risk level of ANSP is high or extremely high, and the water quality level is IV, V and inferior V). The results for 2015 were taken as an example to identify the key areas for risk prevention and control, which mainly include urban areas, but some are also distributed in other areas (Fig. 4). The key control areas are mainly include Yongchuan, Bishan, Shapingba, Jiulongpo and Beibei, etc. The key prevention areas are mainly located in Dazu, Rongchang, Nanchuan, Pengshui and Qianjiang, etc. And involve the Apeng River, Bixi River, Chengbei River, Yutan Reservoir and Yujiang River, *etc*. The key control areas are mainly located in Jiulongpo, Middle of Yongchuan, East of Bishan, Shapingba and Liangping, etc. And involve the Liangtan River, Qijian River, Tiaodeng River, Xiaosha River and Yuanyi River, *etc*.

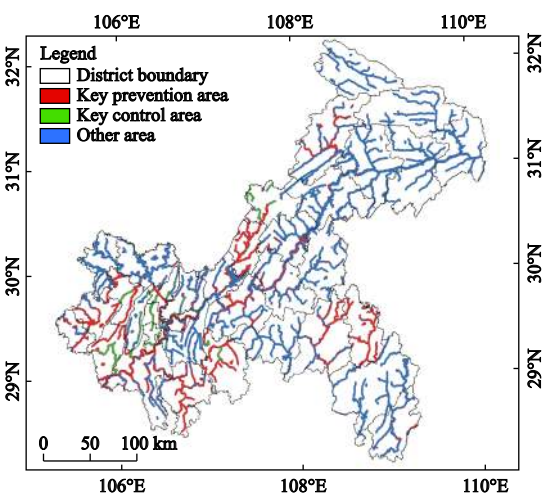

Fig. 4 Distribution of key areas for risk prevention and control in 2015 in Chongqing, China

4 Discussion

In terms of model measurement analysis, the accuracy of measurement results is highly important and represents the basis of measurement model generalization. We conducted a lateral assessment from the perspective of river water quality and explored the influences of different land use types on the risk intensity of ANSP from different rivers, as well as the possible causes of centroid movement in risk regions. We also identified the key areas of risk prevention and control to provide data support for the development of risk prevention and control strategies.

4.1 Accuracy of the risk measurement results by the proposed model

At present, Basnyat et al. (2000), Rabotyagov et al. (2014), Strehmel et al. (2016), WANG et al. (2016), KANG et al. (2018) and WU et al. (2020) have done some model research on the risk measurement of ANSP, while on the whole, the pollution process and influencing factors of ANSP are not fully considered. The ANSP risk assessment model we built comprehensively considers the three processes of pollutant source input, intermediate transformation, and terminal absorption, as well as the key factors that affect the ANSP risk. Although the risk measurement results are based on the analysis of potential threats, theoretically, there is an overall positive correlation between water quality, area of source land and the risk intensity of ANSP (Chen et al., 2018). This has been confirmed by Heiderscheidt et al. (2015), De Oliveira et al. (2017), and Tahmasebi Nasab et al. (2018). Hence, to reflect the accuracy of the risk measurement model constructed by this study, the regions within 1 km on both sides of the river were taken as the model accuracy assessment area, and the spatial correlation between the risk measurement results of the assessment area and the water quality standards of water environment functional area in different periods was analyzed. If there was a positive correlation in all periods, the model was considered effective for reflecting the risk of regional ANSP. In this study, the waveband set statistical tool of the ArcGIS software was used

to conduct spatial correlation analysis on the water quality standards of each river and the risk measurement results for different periods. In all cases, we found a positive correlation, with correlation coefficients of 0.28, 0.30, 0.25, and 0.29 for 2000, 2005, 2010, and 2015, respectively. Therefore, the measurement results provided by the constructed model can well reflect the risk of regional ANSP.

The study further discusses the relationship between the area of source land and the risk measurement results. Combined with the research of Wang et al. (2016), Jing and Zhang (2019) and others, it is considered that there was a greater impact of the source land area on the risk measurement results. Therefore, three rivers were selected to analyze the relationship between source area (land use type) and risk intensity. In this study, we selected the risk measurement results and land use types for 2000 of the main urban areas, northeastern Chongqing, Liangtan River of southeastern Chongqing, Wanzhou section of Ruxi River, and Apeng River for analysis. The regions with higher proportions of high- and extremely high-risk areas had relatively high proportions of river cultivated land and construction land. For example, for the Liangtan River, the proportion of extremely high-risk areas was 78.23%, and the corresponding proportions of cultivated land and construction land were 63.05% and 14.63%, respectively. The regions dominated by medium-risk areas had close proportions of river cultivated land and forest land. For example, in the Wanzhou section of the Ruxi River, medium-risk areas accounted for 45.53%, and the corresponding proportions of cultivated land and forest land were 45.02% and 52.50%, respectively. The regions with higher proportions of low-risk areas showed significantly increased proportions of river forestland and wetland. For example, in the Apeng River, the proportion of low-risk areas was 62.28%, and the corresponding proportions of forestland and wetland were 57.07% and 4.55%, respectively (Table 5). These results lead us to infer that the composition of land use types has an obvious influence on the risk intensity of ANSP, and it was consistent with the result of model calculation.

4.2 Urbanization promotes the movement of the centroid of risk regions

The results show that the centroid of the high-risk, extremely high-risk regions and cultivated land have obvious eastward migration (Fig. 5), and cultivated land is the most obvious spatial feature of urbanization expansion (Jing and Zhang, 2019). By acquiring the spatio-temporal changes in cultivated land occupation (the most obvious characteristic of urbanization) for each period, the relationships between the spatio-temporal changes in cultivated land occupation and the eastward shift of centroids of high- and extremely high-risk regions were analyzed. By measuring the changes in the centroid of cultivated land in each period, we found that the centroid coordinates in 2000, 2005, 2010, and 2015 were (36 456 059, 3 318 275), (36 456 954, 3 316 935), (36 456 433, 33 19 095), and (36 457 998, 3 319 991), respectively. The movement directions of the centroids in 2000−2005, 2005−2010, and 2010−2015 were 56.24°

Table 5 Influences of land use types on ANSP risk intensity in Chongqing, China / %

Type	River	Liangtan River	Wanzhou section of Ruxi River	Apeng River
Proportion of each level of risk	No risk	0	0.05	2.63
	Low risk	0	43.66	62.28
	Medium risk	0	45.53	33.58
	High risk	21.77	10.47	1.5
	Extremely high risk	78.23	0.29	0.01
Proportion of land use types	Grassland	0	0.33	1.56
	Cultivated land	63.05	45.02	36.08
	Forest land	18.79	52.5	57.07
	Other land	0	0	0.62
	Construction land	14.63	0.57	0.12
	Wetland	3.53	1.58	4.55

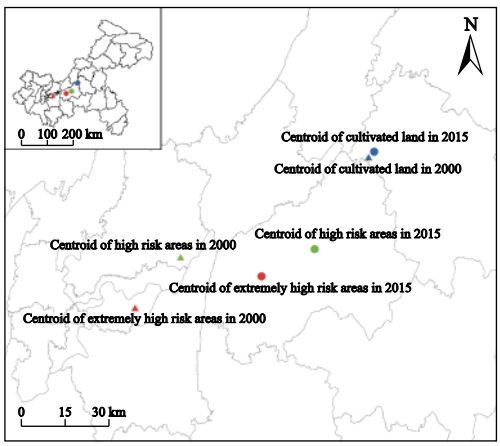

Fig. 5 Movement distribution map of the centroid of high-risk, extremely high-risk areas and cultivated land in Chongqing, China

east by south, 76.44° west by north, and 29.83° east by north, respectively, and the movement velocity values of the centroids in 2000−2005, 2005−2010, and 2010−2015 were 322.24 m/yr, 444.27 m/yr, and 360.64 m/yr, respectively. In the entire period from 2000 to 2015, there was an obvious eastward shift, and the centroid of cultivated land moved to the northeast at a speed of 172.67 m/yr, with a total distance of 2590 m. These results indicate that there is an obvious correlation between cultivated land occupation in the course of urbanization and the eastward shift of the centroid of risk areas, reflecting the decrease in agricultural activity intensity in the main urban areas. This is consistent with the research conclusion of Cheng et al. (2019), which shows that the change of cultivated land area has a greater impact on the spatial change of ANSP risk.

4.3 Proposal

4.3.1 Urban planning should focus on internal upgrading to avoid waste of cultivated land resources

In the process of urbanization, cultivated land is occupied a lot. This situation will undoubtedly increase the regional safety risk of total grain production and the transportation costs of grain. In recent years, China has carried out some protection measures to prevent cultivated land from blind occupation, such as the designation of permanent basic farmland, the reclamation of abandoned land use, etc. (Cheng et al., 2017). However, in the practical survey, there were few permanent delimitated zones of basic farmland surrounding most urban built-up areas, which means that the cultivated land surrounding these areas is likely to be occupied for urbanization in the future. In view of the cultivated land occupied will have an impact on the quality of cultivated land and food security. Our study suggests that urban development in the future should focus on the upgrading of aged and old urban areas rather than on blindly carrying out spatial expansion. This thought is consistent with the idea of green city renewal, proposed by Lin et al. (2019). Similarly, in the urban renewal of the Xigu region of Tianjin, Dong et al. (2016) proposed that the original urban structure should be retained through organic renewal and that the parts not suitable for urban development should be removed, thus creating a more suitable environment for modern life. In the urban organic renewal of Wenzhou, Zhou et al. (2015) proposed to reuse the stock land and renovate the old villages, old factories, and old urban areas based on the perspective of organic renewal and the combination of comprehensive renovation and improvement. The idea of urban organic renewal in these different regions indicates that the thought of strengthening internal upgrading and improvement in prospective urban development has been gradually put into practice, which is conducive to the effective protection and preservation of cultivated land around urban areas.

4.3.2 Risk prevention and control should focus on the agricultural production mode of high-risk and extremelyhigh-risk agglomeration area

High-risk and extremely high-risk concentration areas are the key areas that need to be prevented and controlled from the policy level, especially for chemical fertilizers, pesticides, aquaculture and other aspects, which need to put forward higher requirements to ensure that the ANSP risk is controlled. According to the Chongqing data system (http://www.cqdata.gov.cn/), the amount of chemical fertilizer and pesticide would reach 278.24 kg/ha and 18.45 kg/ha respectively in 2018. Therefore, local government departments should strictly control the increase of fertilizer and pesticide consumption in accordance according to the requirement of "zero growth of fertilizer and pesticide" of the Ministry of Agriculture of China. At the same time, considering that the area of cultivated land is also decreasing, we should ensure that the actual use intensity is not increased while the amount of chemical fertilizer and pesticide is decreased. In addition, the technical promotion and financial support of large-scale breeding should be streng-

thened, and the pollution risk of retail breeding should be gradually reduced.

4.3.3 The reduction ability of ANSP should be enhanced in key regions of prevention and control

The key regions for prevention and control are the areas with high or extremely high ANSP risk, which pose a high threat to local water quality. At present, many studies have proved that the risk of ANSP can be alleviated effectively through constructing vegetation buffer zone and wetland around the water area or watershed outlet (Zhu et al., 2020). At the same time, in the construction of vegetation buffer zone and constructed wetland, the plants with good economic value and landscape value can be selected according to the local natural environment. These plants can not only retain and absorb pollutants, but also provide more value for human beings.

4.4 Further research plan

Because our model integrates panel data, remote sensing data, and statistical data, the research mainly focuses on the existing data, which makes the research unable to well analyze the future risk situation. Therefore, future research will combine CLUE-S (Kucsicsa et al., 2019), CA (Nouri et al., 2014) and other models to simulate future land use types. We will combine the simulation results of land use types with PTA model for future ANSP risk analysis, and to maximize the value of our research.

5 Conclusions

We have established the PTA model of ANSP risk measurement based on the process of "pressure, transformation and absorption", which provides a new method for ANSP risk measurement and is conducive to better carry out the prevention and control of ANSP. Meanwhile, we provide the analysis methods of spatial-temporal evolution for other studies. Based on the water quality status of all rivers, it can be indirectly deduced that the accuracy of the PTA model is in line with the research requirements. This study found that there was an obvious transformation tendency of ANSP risk from low risk to high-risk, and that the risk level in the main urban areas was considerably higher than that in southeastern and northeastern Chongqing, China (The proportion of high-risk and extremely high-risk increased from 17.82% and 16.63% in 2000 to 18.10% and 16.76% in 2015, respectively). The centroids of extremely high-risk, high-risk, medium-risk, low-risk, and no-risk areas all presented a spatial feature of successive distribution from west to east, and the high- and extremely high-risk areas showed an eastward shift (From 2000 to 2015, the centroids of high-risk and extremely high-risk regions moved 4.63 km (1.68°) and 4.48 km (12.08°) east by north, respectively). Kernel density analysis showed that the high-risk level was mainly concentrated in the main urban areas; the overall risk concentration degree of northeastern and southeastern Chongqing was low, albeit with an increasing trend. In the concentrated distribution high- and extremely high-risk areas, on the whole, the spatial fragmentation degree increased, with a tendency to decentralized concentration. The risk intensity was significantly affected by the composition of land use types (area of source land), and the risk level in the regions with higher proportions of cultivated land and artificial surface was significantly increased. In the process of urbanization, the occupation of cultivated land promoted the centroid movement of high-risk and high-risk regions.

Based on the results, it was believed that the decrease of cultivated land reduced the risk of ANSP in metropolitan areas, and the change of cultivated land quantity in high-risk areas should be focused in the future. The government should give priority to the conversion of cultivated land in high-risk areas into woodland, grassland and other types, try to avoid occupying the cultivated land in low-risk areas, and reduce the risk of ANSP from the perspective of optimal layout of cultivated land. In addition, in the risk prevention and control of ANSP, the focus should be on the regions with higher risk concentration degrees and on the key areas for prevention and control. At the same time, we should pay significant attention to the construction of ecological corridors in certain scopes of rivers to improve the proportion of forest areas. In the process of urbanization, we should give priority to internal upgrading and transformation rather than blind surface expansion, and avoid occupation of cultivated land in low-risk areas of ANSP.

References

Basnyat P, Teeter L D, Lockaby B G et al., 2000. The use of remote sensing and GIS in watershed level analyses of non-point source pollution problems. *Forest Ecology and Management*,

128(1–2): 65–73. doi: 10.1016/S0378-1127(99)00273-X

Cai Y P, Rong Q Q, Yang Z F et al., 2018. An export coefficient based inexact fuzzy bi-level multi-objective programming model for the management of agricultural nonpoint source pollution under uncertainty. *Journal of Hydrology*, 557: 713–725. doi: 10.1016/j.jhydrol.2017.12.067

Chen Yuchan, Zhang Zhengdong, Wan Luwen et al., 2018. Identifying risk areas and risk paths of non-point source pollution in Wuhua River Basin. *Acta Geographica Sinica*, 73(9): 1765–1777. (in Chinese)

Cheng Q W, Jiang P H, Cai L Y et al., 2017. Delineation of a permanent basic farmland protection area around a city centre: case study of Changzhou City, China. *Land Use Policy*, 60: 73–89. doi: 10.1016/j.landusepol.2016.10.014

Cheng X, Chen L D, Sun R H, 2019. Modeling the non-point source pollution risks by combing pollutant sources, precipitation, and landscape structure. *Environmental Science and Pollution Research*, 26(12): 11856–11863. doi: 10.1007/s11356-019-04384-y

Chongqing Market Supervision and Administration Bureau, 2019. DB50/T 931−2019 Technical specification for risk evaluation of agricultural non-point source. Chongqing: Chongqing Market Supervision and Administration Bureau. (in Chinese)

De Oliveira L M, Maillard P, Pinto E J D A, 2017. Application of a land cover pollution index to model non-point pollution sources in a Brazilian watershed. *CATENA*, 150: 124–132. doi: 10.1016/j.catena.2016.11.015

Dong Jun, Gao Yan, Han Dongsong, 2016. Organic renovation of old district from security viewpoint: Xigu Area, Tianjin. *Planners*, 32(3): 47–53. (in Chinese)

Heiderscheidt E, Leiviskä T, Kløve B, 2015. Chemical treatment response to variations in non-point pollution water quality: results of a factorial design experiment. *Journal of Environmental Management*, 150: 164–172. doi: 10.1016/j.jenvman.2014.10.021

Hou X Y, Ying L L, Chang Y Y et al., 2014. Modeling of non-point source nitrogen pollution from 1979 to 2008 in Jiaodong Peninsula, China. *Hydrological Processes*, 28(8): 3264–3275. doi: 10.1002/hyp.9886

Jiang Qian, Sun Weilin, Zhu Lizhi, 2018. Analysis of temporal and spatial variations of nutrient balance and its environmental risk in Zhejiang Province. *Resources and Environment in the Yangtze Basin*, 27(2): 335–344. (in Chinese)

Jing Yande, Zhang Huamei, 2019. Risk assessment of non-point source pollution output in Nansihu Lake Basin based on LUCC. *Journal of Natural Resources*, 34(1): 128–139. (in Chinese). doi: 10.31497/zrzyxb.20190111

Kang Zhiming, Zhang Rongxia, Ye Yuzhen et al., 2018. GIS-based pollution risk assessment of nitrogen and phosphorus loss in surface runoff in farmlands in Fujian Province. *Chinese Journal of Eco-Agriculture*, 26(12): 1887–1897. (in Chinese)

Karandish F, Šimůnek J J, 2014. Two-dimensional modeling of nitrogen and water dynamics for various N-managed water-saving irrigation strategies using HYDRUS. *Agricultural Water Management*, 193: 174–190. doi: 10.1016/j.agwat.2017.07.023

Kristan M, Leonardis A, 2014. Online discriminative kernel density estimator with Gaussian kernels. *IEEE Transactions on Cybernetics*, 44(3): 355–365. doi: 10.1109/TCYB.2013.2255983

Kucsicsa G, Popovici E A, Bălteanu D et al., 2019. Future land use/cover changes in romania: regional simulations based on CLUE-S model and CORINE land cover database. *Landscape and Ecological Engineering*, 15(1): 75–90. doi: 10.1007/s11355-018-0362-1

Li J, Zhai C Z, Yu J Y et al., 2018. Spatiotemporal variations of ambient volatile organic compounds and their sources in Chongqing, a mountainous megacity in China. *Science of the Total Environment*, 627: 1442–1452. doi: 10.1016/j.scitotenv.2018.02.010

Li Yuechen, Liu Chunxia, Min Jie et al., 2013. RS/GIS-based integrated evaluation of the ecosystem services of the Three Gorges Reservoir area (Chongqing section). *Acta Ecologica Sinica*, 33(1): 168–178. (in Chinese). doi: 10.5846/stxb201107020989

Lin Jian, Ye Zijun, 2019. Green urban renewal: an important direction for urban development in the new era. *City Planning Review*, 43(11): 9–12. (in Chinese)

Liu Chenfeng, Wang Zhifeng, Zhao Xingzheng et al., 2020. Evaluation of land carrying capacity of livestock and poultry manure nitrogen based on the Second China Pollution Source Census Results. *Research of Environmental Sciences*, 33(12): 2657–2664. (in Chinese)

Liu Chunxia, Zhu Kangwen, Li Yuechen, 2017. Research on the urban expansion in Chengdu-Chongqing Economic Zone Based on DMSP/OLS nighttime light data in recent 20 years. *Journal of Chongqing Normal University (Natural Science)*, 34(6): 117–126. (in Chinese)

Liu G D, Wu W L, Zhang J, 2005. Regional differentiation of non-point source pollution of agriculture-derived nitrate nitrogen in groundwater in northern China. *Agriculture, Ecosystems & Environment*, 107(2–3): 211–220. doi: 10.1016/j.agee.2004.11.010

Liu Qinpu, 2014. Distribution of fertilizer application and its environmental risk in different provinces of China. *Scientia Agricultura Sinica*, 47(18): 3596–3605. (in Chinese)

Mao Zhanpo, Yin Chengqing, Shan Baoqing et al., 2002. Multi-factor model for analyzing the regulation effect of wetland area on storm runoff. *Journal of Hydraulic Engineering*, (7): 57–63. (in Chinese)

Ministry of Agriculture and Rural Affairs of the People's Republic of China.*Technical guide for calculating the carrying capacity of livestock and poultry manure*. available at http://www.moa.gov.cn/govpublic/XMYS/201801/t20180122_6135486.htm. (2018-01-15) (in Chinese)

Nouri J, Gharagozlou A, Arjmandi R et al., 2014. Predicting urban land use changes using a CA-Markov model. *Arabian Journal for Science and Engineering*, 39(7): 5565–5573. doi: 10.1007/s13369-014-1119-2

Okabe A, Satoh T, Sugihara K, 2009. A kernel density estimation method for networks, its computational method and a GIS-based tool. *International Journal of Geographical Information Science*, 23(1): 7–32. doi: 10.1080/13658810802475491

Ouyang W, Huang H B, Hao F H et al., 2012. Evaluating spatial interaction of soil property with non-point source pollution at watershed scale: the phosphorus indicator in Northeast China. *Science of the Total Environment*, 432: 412–421. doi: 10.1016/j.scitotenv.2012.06.017

Ouyang Z Y, Zheng H, Xiao Y et al., 2016. Improvements in ecosystem services from investments in natural capital. *Science*, 352(6292): 1455–1459. doi: 10.1126/science.aaf2295

Ouyang Zhiyun, Wang Qiao, Zheng Hua et al., 2014. National Ecosystem Survey and Assessment of China (2000–2010). *Bulletin of Chinese Academy of Sciences*, 29(4): 462–466. (in Chinese)

Rabotyagov S S, Valcu A M, Kling C L, 2014. Reversing property rights: practice-based approaches for controlling agricultural nonpoint-source water pollution when emissions aggregate nonlinearly. *American Journal of Agricultural Economics*, 96(2): 397–419. doi: 10.1093/ajae/aat094

Shen Z Y, Gong Y W, Li Y H et al., 2009. A comparison of WEPP and SWAT for modeling soil erosion of the Zhangjiachong Watershed in the Three Gorges Reservoir Area. *Agricultural Water Management*, 96(10): 1435–1442. doi: 10.1016/j.agwat.2009.04.017

Smith L E D, Siciliano G, 2015. A comprehensive review of constraints to improved management of fertilizers in China and mitigation of diffuse water pollution from agriculture. *Agriculture, Ecosystems & Environment*, 209: 15–25. doi: 10.1016/j.agee.2015.02.016

Strand J, Carson R T, Navrud S et al., 2017. Using the Delphi method to value protection of the Amazon rainforest. *Ecological Economics*, 131: 475–484. doi: 10.1016/j.ecolecon.2016.09.028

Strehmel A, Schmalz B, Fohrer N, 2016. Evaluation of land use, land management and soil conservation strategies to reduce non-point source pollution loads in the Three Gorges Region, China. *Environmental Management*, 58(5): 906–921. doi: 10.1007/s00267-016-0758-3

Sun Cheng, Zhou Huazhen, Chen Lei et al., 2017. The pollution risk assessment of nitrogen and phosphorus loss in surface runoff from farmland fertilizer. *Journal of Agro-Environment Science*, 36(7): 1266–1273. (in Chinese)

Sun Fan, Feng Shenping, Xiao Qiang, 2014. Research on urban and rural ecological civilization construction from the view of scientific outlook on development-taking the Pengshui county of the Chongqing city as an example. *Journal of Southwest University (Natural Science Edition)*, 36(12): 101–106. (in Chinese)

Tahmasebi Nasab M, Grimm K, Hadi Bazrkar M et al., 2018. Swat modeling of non-point source pollution in depression-dominated basins under varying hydroclimatic conditions. *International Journal of Environmental Research and Public Health*, 15(11): 2492. doi: 10.3390/ijerph15112492

Wang G Q, Li J W, Sun W C et al., 2019. Non-point source pollution risks in a drinking water protection zone based on remote sensing data embedded within a nutrient budget model. *Water Research*, 157: 238–246. doi: 10.1016/j.watres.2019.03.070

Wang J L, Shao J A, Wang D et al., 2016. Identification of the "source" and "sink" patterns influencing non-point source pollution in the Three Gorges Reservoir Area. *Journal of Geographical Sciences*, 26(10): 1431–1448. doi: 10.1007/s11442-016-1336-6

Wang Junneng, Zhao Xuetao, Cai Nan et al., 2020. Pollution discharge and environmental treatment efficiency of rural domestic sewage in China. *Research of Environmental Sciences*, 33(12): 2665–2674. (in Chinese)

Wang Lei, Xiang Bao, Su Benying et al., 2017. Spatial-temporal variation of agricultural non-point source pollution risk in Beijing-Tianjin-Hebei Region, China. *Journal of Agro-Environment Science*, 36(7): 1254–1265. (in Chinese)

Wang Q, Zambom Z A, 2019. Subsampling-extrapolation bandwidth selection in bivariate kernel density estimation. *Journal of Statistical Computation and Simulation*, 89(9): 1740–1759. doi: 10.1080/00949655.2019.1597099

Williams J R, Renard K G, Dyke P T, 1983. EPIC: a new method for assessing erosion's effect on soil productivity. *Journal of Soil and Water Conservation*, 38(6): 381–383.

Wu Hanqing, Wan Wei, Shan Yanjun et al., 2020. Environmental risk assessment of phosphorus loss from farmland based on phosphorus index model in the Haihe River Basin. *Transactions of the Chinese Society of Agricultural Engineering*, 36(14): 17–27. (in Chinese)

Wu Jiansheng, Liu Hao, Peng Jian et al., 2014. Hierarchical structure and spatial pattern of China's urban system: evidence from DMSP/OLS nightlight data. *Acta Geographica Sinica*, 69(6): 759–770. (in Chinese)

Xiao Qin, Zhou Zhenya, Luo Qiyou, 2019. Bearing capacity assessment and forewarning analysis of livestock and poultry breeding in the middle and lower reaches of Yangtze River. *Resources and Environment in the Yangtze Basin*, 28(9): 2050–2058. (in Chinese)

Xu Z A, Li T, Bi J et al., 2018. Spatiotemporal heterogeneity of antibiotic pollution and ecological risk assessment in Taihu Lake Basin, China. *Science of the Total Environment*, 643: 12–20. doi: 10.1016/j.scitotenv.2018.06.175

Zhang Fusuo, Wang Jiqing, Zhang Weifeng et al., 2008a. Nutrient use efficiencies of major cereal crops in china and meas-

ures for improvement. *Acta Pedologica Sinica*, 45(5): 915–924. (in Chinese)

Zhang Jiaqi, Ge Yong, Wu Yijin et al., 2016. Analysis on the evolution of ecological security pattern in Wuling Mountain. *Journal of Geo-information Science*, 18(3): 315–324. (in Chinese)

Zhang Qianzhu, Wang Tongtong, Lu Yang et al., 2019. Regionalization of torrential flood disasters in Chongqing based on AHP-GIS. *Resources and Environment in the Yangtze Basin*, 28(1): 91–102. (in Chinese)

Zhang Weifeng, Ji Yuexiu, Ma Ji et al., 2008b. Driving forces of fertilizer consumption in China (Ⅱ planting structure). *Resources Science*, 30(1): 31–36. (in Chinese)

Zhong Jing, Lu Tao, 2018. Optimal statistical unit for relief amplitude in Southwestern China. *Bulletin of Soil and Water Conservation*, 38(1): 175–181, 186. (in Chinese)

Zhou J, Wu Y H, Wang X X et al., 2019. Divergent patterns of soil phosphorus discharge from water-level fluctuation zone after full impoundment of Three Gorges Reservoir, China. *Environmental Science and Pollution Research*, 26(3): 2559–2568. doi: 10.1007/s11356-018-3805-1

Zhou Wufu, Ge Lingniao, Xie Jichang, 2015. Urban renewal planning strategies from organic renewal viewpoint, Wenzhou. *Planners*, 31(5): 105–112. (in Chinese)

Zhu Jin, Zhu Weihong, Jin Ri et al., 2019. Health evaluation of wetland ecosystems in Tumen River Basin in China. *Wetland Science*, 17(3): 344–351. (in Chinese)

Zhu K W, Chen Y C, Zhang S et al., 2020. Vegetation of the water-level fluctuation zone in the Three Gorges Reservoir at the initial impoundment stage. *Global Ecology and Conservation*, 21: e00866. doi: 10.1016/j.gecco.2019.e00866

Zuo Taian, Su Weici, Ma Jingna et al., 2010. Ecological security of land evaluation in the Three Gorges Reservoir Area of Chongqing for water and soil erosion. *Journal of Soil and Water Conservation*, 24(2): 74–78. (in Chinese)